Tetrahedron Letters 56 (2015) 4871–4876

Contents lists available at ScienceDirect

Tetrahedron Letters

journal homepage: www.elsevier.com/locate/tetlet

Synthesis of gold nanoparticles using electron-donating dithiafulvene units

Anabel E. Lanterna [a,†], Eduardo A. Coronado [b], Alejandro M. Granados [a,*]

[a] Instituto de Investigaciones en Fisicoquímica de Córdoba (INFIQC-CONICET), Departamento de Química Orgánica, Facultad de Ciencias Químicas—Universidad Nacional de Córdoba, Ciudad Universitaria (X5000HUA)—Córdoba, Argentina
[b] Departamento de Fisicoquímica, Facultad de Ciencias Químicas—Universidad Nacional de Córdoba, Ciudad Universitaria (X5000HUA)—Córdoba, Argentina

ARTICLE INFO

Article history:
Received 27 May 2015
Revised 18 June 2015
Accepted 22 June 2015
Available online 26 June 2015

Keywords:
Gold nanoparticle
Dithiafulvene
Reducing agent
Capping agent

ABSTRACT

Dithiafulvene (DTF) derivative compounds were used as reducing agents to synthesize capped gold nanoparticles (AuNPs). DTF derivatives had shown good capability to reduce Au(III) to Au(0) without further addition of common reducing agents, and at the same time they were able to act as good capping agents. Because of their spectroscopic characteristics we were able to follow the AuNP formation by UV–Vis spectroscopy. Raman and NMR experiments were also performed in order to estimate the composition of the final capped AuNP species.

Introduction

Gold nanoparticles (AuNPs) feature a wide range of potential applications in fields such as medicine,[1] biotechnology[2] and catalysis,[3] and are thus among the most intensely studied nanoscale materials.[4] AuNPs can be prepared via various synthetic routes including chemical, sonochemical or photochemical approaches.[5] The most common chemical procedure for the synthesis in aqueous solution is the reduction of a dissolved gold precursor, for example HAuCl4, by a reducing agent such as sodium citrate, ascorbic acid, sodium borohydride ($NaBH_4$) or block copolymers.[6] On the other hand, the synthesis in organic medium was also developed since the first report by Brust et al.[7,8] Formation of AuNPs via the reduction of $HAuCl_4$ in the presence of the thiol ligand has been a widely used technique in preparing ligand-stabilized AuNPs. In this sense, the Brust–Shiffrin two-phase method (BSM) is the most popular method to prepare organic ligands (mostly thiolate) stabilized AuNPs.[8] Schiffrin and co-workers proposed a two-step mechanism for the formation of AuNPs from $HAuCl_4$. The first step involves the conversion of Au(III) salt to the Au(I) state (as thiolate salt). The second step involves the reductive decomposition of the polymeric Au(I) thiolate to form AuNPs by the addition of a reducing agent as $NaBH_4$.[9]

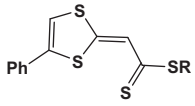

Scheme 1. 1,3-Dithiol-2-ylidene rings, or dithiafulvenes (DTF) used as reducing and capped agent as well. R = alkyl groups.

The dithiafulvene unit (1,3-dithiole-2-ylidene group Scheme 1) is a good electron donor used in the design and synthesis of new organic materials, especially in the search for extended tetrathiafulvalene derivatives.[10]

DTF are widely used for switchable processes, furthermore they are also found as part of push–pull donor–acceptor dyads and cruciforms with unprecedented non-linear optical and redox-controlled characteristics.[11] Those interesting electronic properties can be explained by their resonance structures in the ground state (Scheme 2).

DTF are able to interact with ions, metal surfaces, metal carbonyl fragments,[12] and they could also reduce metal ions according to the redox potential reported.[13] Andreu et al.[14] have informed the redox potential for different 6,6-disubstituted 1,4-dithiafulvenes varying from −1.50 to −1.20 V (in CH_2Cl_2 vs Ag/AgCl) when stronger electron-withdrawing groups are used.

* Corresponding author.
E-mail address: ale@fcq.unc.edu.ar (A.M. Granados).
† Present address: Centre for Catalysis Research and Innovation, Department of Chemistry and Biomolecular Sciences, Faculty of Sciences, University of Ottawa, Canada.

http://dx.doi.org/10.1016/j.tetlet.2015.06.064
0040-4039/

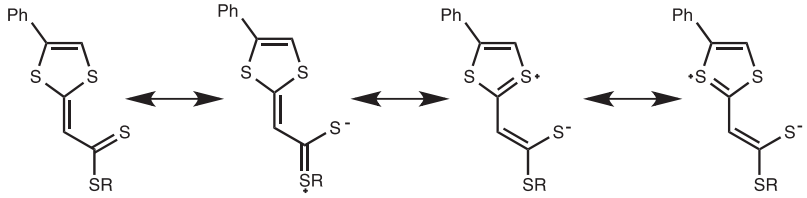

Scheme 2. 1,3-Dithiol-2-ylidene rings ground state resonance structures.

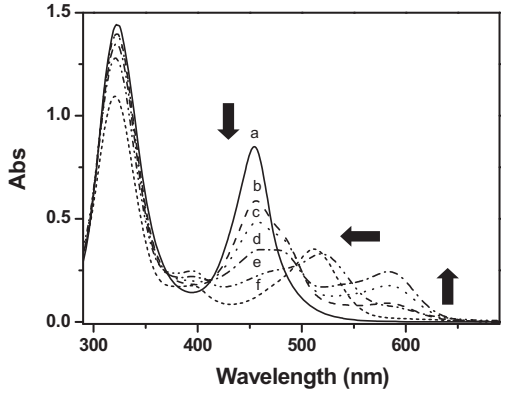

Figure 1. Spectra of the mixture of $HAuCl_4$ and DTF at 48 °C (C_{Au}/C_{DTF}: 10) after (a) 0 min; (b) 60 min; (c) 120 min; (d) 330 min; (e) 1360 min; and (f) 7130 min.

Thus, they could be used on the reduction of $AuCl_4^-$ to Au^0 (0.99 V vs SHE).[15] In this work, we present the capacity of DTF molecules to reduce Au(III) leading to stable AuNPs capped with DTF oxidized species (AuNP@DTF_{ox}). The synthesis of these particles in MeCN is described using different concentrations of both Au(III) (C_{Au}) and DTF (C_{DTF}). The AuNPs have shown great stability in the colloidal dispersion, and they can also be resuspended in solvents of different polarities such as water and toluene, a feature very useful for different applications. A kinetic study using UV–Vis spectroscopy has been also performed. The analysis of the evolution of the different UV–Vis bands evidences the presence of an intermediate attributed to DTF oxidized species formed during the redox process. A critical amount of this intermediate is necessary to achieve the AuNP formation. Additional experiments using Raman and ^1H NMR spectroscopy at different stages during AuNP formation give further indications about the structure of the oxidized DTF covering AuNPs.

Results and discussion

The AuNPs formed at different C_{Au}/C_{DTF} were a well stable colloid solution of AuNP@DTF_{ox} in MeCN. Droplets of this suspension analysed by TEM showed particles with different shapes and sizes depending on the reaction time in which they were collected. These colloids can easily be transferred to aqueous solution by evaporation of the organic solvent (Fig. S1) and could be extracted from water with toluene (Fig. S2). In all cases, the colloids showed great stability for several weeks.

In order to study the ability of DTF as reducing agent, the synthesis of AuNP@DTF_{ox} has been performed with solutions at different C_{Au}/C_{DTF} (see Table S1). The UV–Vis spectrum of pure DTF compounds in MeCN depicts two characteristic absorption peaks, the first one at ~350 nm, due to the π–π^* transition, and the second one at 454 nm corresponding to the n–π^* transition of the DTF. After mixing with the metal precursor the band at 454 nm decreases while another band at 485 nm emerges (Fig. 1). We attributed this process (ad hoc) to the oxidation of the DTF and the possible formation of a complex between the oxidized DTF and Au(I) (DTF_{ox}–Au(I)), respectively (vide infra). After this complex has reached a certain concentration, another band centred at 580 nm appears, which is associated to the Localized Surface Plasmon Resonance (LSPR) of an anisotropic shaped AuNP (see inset in Fig. 2). The gradual blue-shifts of this band observed after five days of reaction (Fig. 1) are consistent with the formation and reshaping of the anisotropic AuNPs to spherical ones (confirmed by TEM). These morphological changes could be related to the thermodynamic control of the shape and size of the particle formation. Experiments performed at different C_{Au}/C_{DTF} show almost the same general features (cf. Figs. 1, S3 and S4).

Up to this point, the results showed DTF was able to reduce the Au(III) to form AuNPs without any additional reducing agent. The kinetic of the formation of AuNPs was studied by UV–Vis spectroscopy at different temperatures and C_{Au}/C_{DTF}; and analysed at two different stages (Fig. 6). The first stage of the reaction analysed between 0 and 125 min after mixing of the reactants involves a

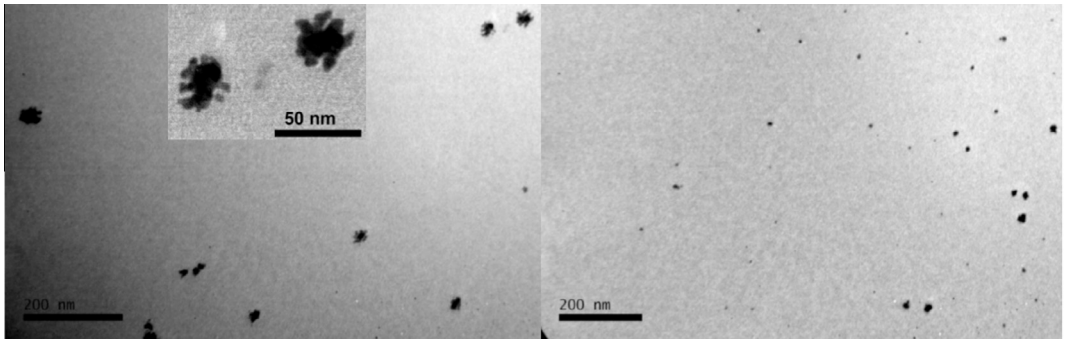

Figure 2. TEM images of AuNP@DTF_{ox} (C_{Au}/C_{DTF}: 10). Left: after two hours of reaction only coral shape particles of around 50 nm were found. Right: after five days of reaction a mixture of spherical AuNPs of ca. 5–10 nm and coral shape NP of around 30–40 nm were observed (reshaping).

decrease of the band at 454 nm, along with the formation of a band at 485 nm (DTF_{ox}–Au(I)). Interestingly, there is an isosbestic point at 469 nm which suggests one step for the transformation of DTF to the intermediate (Fig. 3, left). Note that, in case that another intermediate exists, its concentration is undetectable within the detection limits of this technique. In the second stage of the reaction, between 133 and 1200 min, the band at 485 nm decreases and the band at 580 nm (the LSPR band) emerges causing a second isosbestic point around 510 nm. Again, this suggests that the conversion from the intermediate into the AuNPs should take place in only one step. Figure 4 shows the time evolution of the absorption at 454, 485 and 580 nm; corresponding to the maximum absorption wavelength of DTF, DTF_{ox}–Au(I) and AuNP@DTF_{ox}, respectively. Noticeably, there is a threshold concentration of DTF_{ox}–Au(I) needed to observe the formation of the LSPR band of the AuNP@DTF_{ox}. This concentration could be achieved at different times depending on the C_{DTF}/C_{Au} and the temperature (Fig. S5). In the case of C_{DTF}/C_{Au} equal to 2.5, it takes place after ~20 min, as it can be observed in Figure 4.

The dependency of temperature and concentration ratio influences on the formation of the intermediate was likewise evaluated. The spectra were recorded before the appearance of the band at 580 nm where only the formation of the DTF_{ox}–Au(I) intermediate is detected. Assuming a stoichiometry of 1:1 between Au(III) and DTF (see SI), the reaction could be described by Eq. (1).

$$\mathrm{Au(III)} + \mathrm{DTF} \rightarrow \mathrm{DTF_{ox}} - \mathrm{Au(I)} \quad (1)$$

Table 1
Rate constants (k_{obs}) obtained under pseudo-first order conditions at different concentrations and temperatures

	C_{Au}/C_{DTF}	$C_{Au(III)}$ (μM)	λ (nm)	k_{obs} (10^{-5} s^{-1})
i	10[a]	100	454	7.0 ± 0.9
			485	6.4 ± 0.7
ii	15[a]	150	454	10 ± 1
			485	14 ± 2
iii	20[a]	200	454	17 ± 2
			485	25 ± 2
iv	30[a]	300	454	20 ± 3
			485	37 ± 4
v	35[a]	350	454	33 ± 5
			485	53 ± 6
vi	10[b]	100	456	20 ± 3
			485	15 ± 2
vii	10[c]	100	456	120 ± 30
			485	50 ± 30

C_{DTF}: 10 μM.
[a] 20 °C.
[b] 27 °C.
[c] 48 °C.

If the above reaction takes place under pseudo-first order condition, for example by using an excess of Au(III), the apparent kinetic constant (k_{obs}) of this step of the reaction could be estimated (Table 1 and SI for further kinetic discussion[16]).

The data recorded in Table 1 show good agreement between the k_{obs} for the decay of the DTF compound (absorbance at 454 nm)

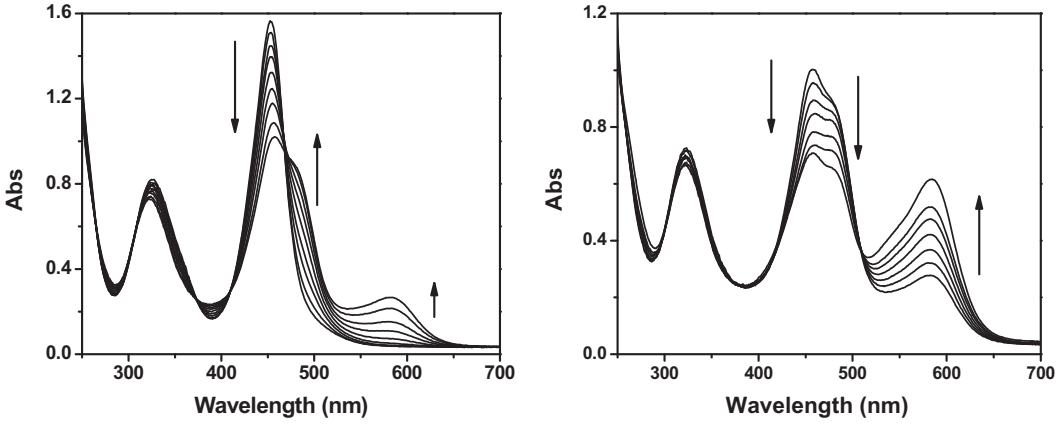

Figure 3. Spectra evolution of the C_{DTF}/C_{Au}: 2.5 in MeCN at 48 °C. Left: Spectra from 0 to 125 min. Note the isosbestic point at 469 nm. Right: Spectra from 133 to 1200 min. Note the isosbestic point at 510 nm.

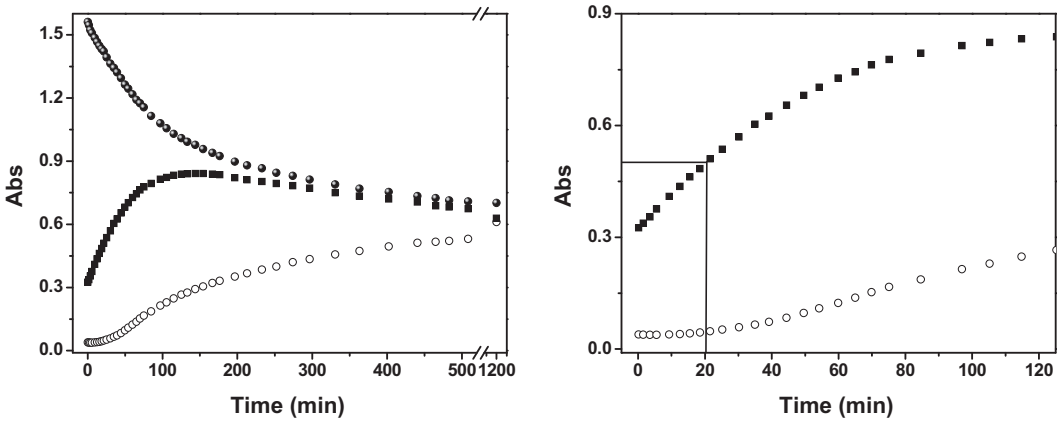

Figure 4. Time evolution of the absorption at (●) 454 nm, (■) 485 nm and (○) 580 nm (C_{DTF}/C_{Au}: 2.5; MeCN (1% H_2O), 48 °C). Right: zoom in the left graph.

$$Au(III) + DTF \rightarrow DTF_{ox} - Au(I)\ complex$$

$$3\ DTF_{ox} - Au(I)\ complex \rightarrow 3\ DTF_{ox} + 2\ Au(0) + Au(III)$$

$$Au(0) \rightarrow\rightarrow AuNP@DTF_{ox}$$

Scheme 3. Mechanism proposed for the AuNP@DTFox synthesis.

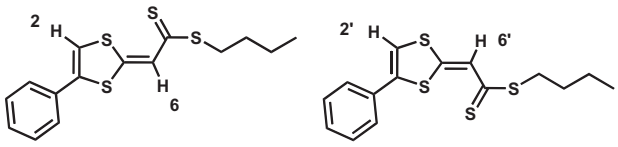

Scheme 4. *E* (left) and *Z* (right) isomers of DTF.

and for the growth of the DTF_{ox}–Au(I) intermediate (absorbance at 485 nm) in the cases where the $C_{Au(III)}$ is low enough (entries i, ii and vi). This is in agreement with the fact that the intermediate is formed from DTF in one step, and explains the isosbestic point observed. On the other hand, at higher $C_{Au(III)}$ (entries iii, iv, v), or at higher temperatures (entry vii), the first step of the reaction becomes more difficult to study, which is reflected by the difference between the k_{obs} obtained. Under these conditions the formation of AuNPs has been accelerated and the separation of the two processes becomes more difficult (see SI Fig. S5). This is in agreement with the several effects that affect the disproportionation of Au(I), such as the temperature and the excess of Au(III).[17] According with these results, the mechanism of the formation of $AuNP@DTF_{ox}$ could be a multiple-step process and involve at least these two steps (Scheme 3): the initial step is the reduction of Au(III) by DTF to form a DTF_{ox}–Au(I) complex. The second step is the disproportionation of aurous species to gold atoms and it was observed even at room temperature, or lower (15 and 20 °C). The disproportionation step combines three Au atoms. This may be promoted by the oxidized DTF species, which play the role of organizer through the formation of the complex that we were able to follow by UV–Vis spectroscopy. At this point, the mechanism of the reduction of Au(III) with DTF could be compared to the synthesis of AuNPs using citrate[18] rather than the mechanism involving thiol protected AuNP synthesis (BSM).[19] Thus, likewise citrate, using DTF the AuNPs can be obtained in homogeneous medium without addition of any other reducing compound due to its dual function as reducing and capping agent.

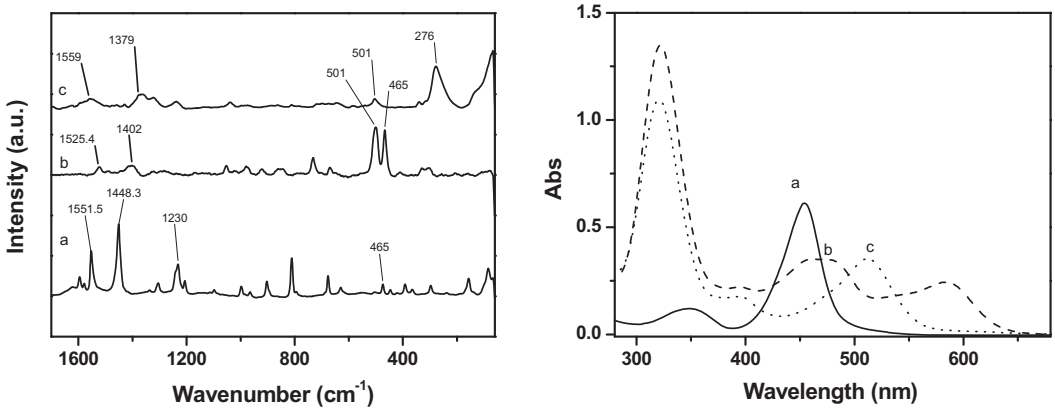

Figure 5. Left: Raman spectrum of the DTF in solid state (a) and SERS spectra obtained after five hours (b) and five days (c) of reaction for solution in entry iii, Table S1. Right: UV–Vis spectra of DTF in MeCN (a), solution in entry iii, Table S1 after five hours (b) and five days (c) of reaction.

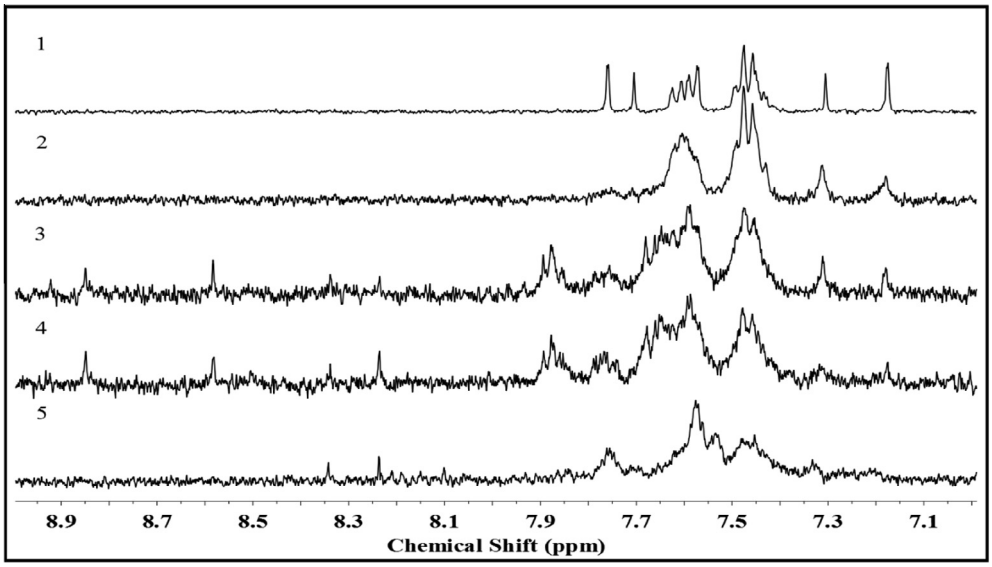

Figure 6. ^1H NMR spectra of: (1) 1.25 mM DTF in MeCN-d_3, (2) DTF solution few minutes after addition of $HAuCl_4$, (3) 2 h 25 min, (4) 5 h 44 min and (5) 66 h. Temperature: 40 °C.

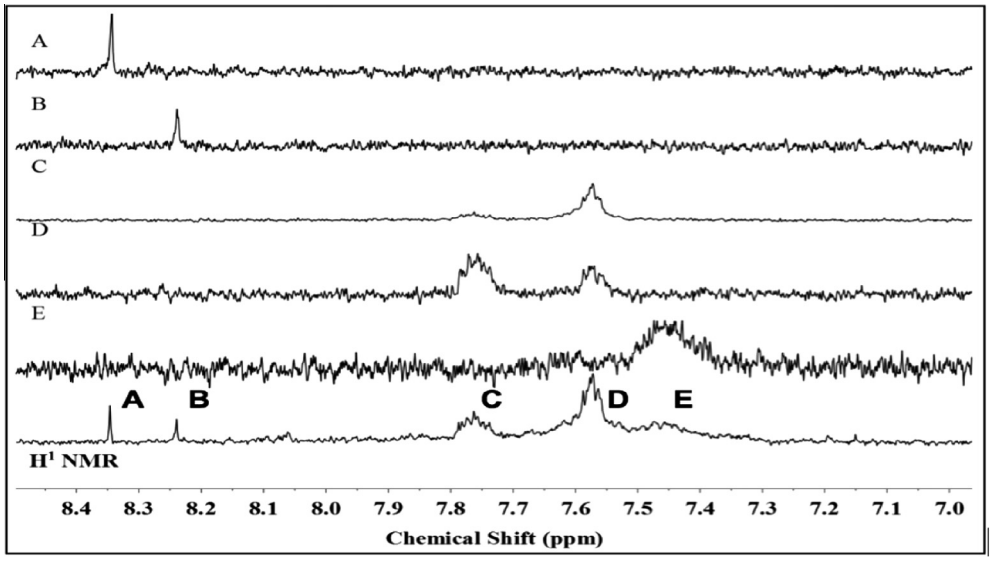

Figure 7. ^{1}H NMR spectrum obtained after 66 h of reaction between DTF and $HAuCl_4$ (C_{DTF}/C_{Au}: 2). Signals are labelled to their identification in the selective TOCSY experiment.

In order to characterize these nanoparticles, we performed SERS spectra of AuNPs (C_{Au}/C_{DTF}: 10) five hours and five days after mixing DTF and $HAuCl_4$. These spectra were compared with the Raman spectrum of pure DTF (Fig. 5). First, we noticed the bands at 1551.5 and 1448.3 cm^{-1} in Raman spectrum of pure DTF (a) assigned to C=C stretching and C–C aromatic ring stretching, respectively, are shifted in spectra (b) and (c) keeping the same intensity ratio. Thus, the aromatic ring seems to be preserved in the final oxidized DTF species. Second, spectrum b shows the coexistence of both DTF (band at 465 cm^{-1}) and oxidized DTF species (band at 501 cm^{-1}) at the AuNP surface. After five days of reaction the band at 465 cm^{-1} has completely disappeared, suggesting only oxidized DTF species remain at the surface. This is further supported by the UV–Vis spectrum obtained at the same time. Finally, spectrum c also shows a strong band at 276 cm^{-1} that was assigned to the Au–S stretching.[20]

The reaction was also performed in MeCN-d_3 at 40 °C and monitored by ^{1}H NMR until no changes were observed (ca. 72 h). The ^{1}H NMR spectrum of the pure DTF is shown in Figure S6. After mixing with the metal precursor, the aromatic region showed the most significant changes during the reaction (Fig. 6). Concisely, few minutes after the addition of $HAuCl_4$ to the DTF solution H2 signals completely disappeared (δ 7.76 *y* 7.70). In addition, signals corresponding to H15-19 lost resolution (broadening). After 2.5 h of reaction H6 signals became too small and they are fused into the noise. On the other hand, the aliphatic region (Fig. S7) shows a splitting of H12 and H13 signals, which suggests the butyl moiety remains and two isomers could be present. It is known this kind of DTF can easily isomerize in solution,[21] therefore the resulting compound structure can also have different isomeric forms. With the aim to get more structure information of the resulting protected AuNPs, selective TOCSY experiments were performed. A 1.25 mM solution of pure DTF in MeCN-d_3 was carried out under selective TOCSY experiments. In this condition, DTF can be in two isomer forms, *E* and *Z*, as it is shown in Scheme 4. Briefly, when the H2 signal (or H6 signal) is irradiated, two signals appearing in the TOCSY spectrum, one belongs to the irradiated H and the other one to the H coupled by W coupling,[22] which is only observed in *E* isomer. As it was expected the spectrum resulting in irradiation of H2′ and H6′ signals (Z isomer) only presents one signal due to the uncoupling system (Fig. S8). The same procedure was performed with a blend of DTF and $HAuCl_4$ (C_{DTF}/C_{Au}: 2) following the reaction for 66 h (Fig. 7, bottom). Selective TOCSY spectra were obtained after irradiation of each signal A, B, C, D and E and collected in Figure 7 (spectra A to E). Only signals C and D were coupled. Other experiment, not shown here (selective COSY experiment), indicates that this is a short scalar coupling, which can take place in the remaining aromatic ring. Accordingly, the results suggest the resulting molecule structure has lost the W coupling at all.

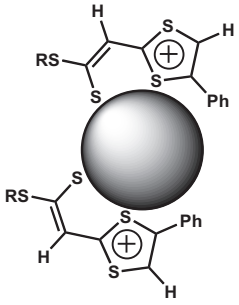

Scheme 5. Suggested structure of AuNPs@DTF_{ox}.

Considering the analysis of the Raman and ^{1}H NMR spectra precedent, on the one hand a plausible structure of the oxidized DTF_{ox} (*Z* isomer) could be as shown in Scheme 5. Another possibility would be that both *E* and *Z* DTF_{ox} isomers interact with the surface of the nanoparticle, and the lack of coupling can be due to the proximity of the dithioate to the gold surface and therefore the expected ionization of the structure. The remainder coupling between protons of the phenyl ring is observed because it occupies a far position from the surface of the gold nanoparticle, where there is a lower interaction.[‡]

Beyond what is the exact explanation of the lack of coupling, it is clear, according to all spectroscopic data, that DTFox has not lost its molecular identity which remains very similar to its predecessor.

Conclusions

We developed a new method to synthesize capped AuNPs using dithiafulvene derivate compounds as a reducing agent. These

[‡] This possibility was suggested by a reviewer.

compounds demonstrated to have a strong capability to reduce Au(III) to Au(0), and reach AuNPs without addition of any other reducing agent. At the same time, these DTF derivative compounds can act as a passivant agent of the NPs formed. We were able to study some aspects of the mechanism involved in the AuNPs formation by UV–Vis spectroscopy. We found the formation of AuNPs takes place after a threshold concentration of the DTF_{ox}–Au(I) is reached. The DTF behaviour during NP formation could be compared with the role of citrate previously described.[18] It is fascinating how the bottom-up synthesis of nanoparticles has been followed by UV–vis spectroscopy as easy as we can follow a regular molecular reaction, thanks to the spectroscopic changes of DTF. The intrinsic properties of DTF and its derivative species suggest the capped AuNPs obtained by this method have potential applications in the electronic field. Additionally, some preliminary results indicate DTF redox ability can also be extended to other metal ions, such as Ag^{+} and Pd^{2+}, generating either homogeneous or supported NPs.

Acknowledgments

This research was supported in part by the Consejo Nacional de Investigaciones Científicas y Técnicas (CONICET); Agencia Nacional de Promoción Científica y Técnica ANPCyT, FONCYT, PME 2006-1544 and SECyT-Universidad Nacional de Córdoba, Argentina. A.E.L. was a grateful recipient of a fellowship from CONICET.

Supplementary data

Supplementary data associated with this article can be found, in the online version, at http://dx.doi.org/10.1016/j.tetlet.2015.06.064.

References and notes

1. Kumar, A.; Zhang, X.; Liang, X.-J. *Colloids Surf., B* **2013**, *107*, 27.
2. Giljohann, D. A.; Seferos, D. S.; Daniel, W. L.; Massich, M. D.; Patel, P. C.; Mirkin, C. A. *J. Phys. Chem. C* **2015**, *119*, 8876.
3. Kyriakou, G.; Beaumont, S. K.; Humphrey, S. M.; Antonetti, C.; Lambert, R. M. *Nanoscale Res. Lett.* **2013**, *8*, 70.
4. Coronado, E. A.; Encina, E. R.; Stefani, F. D. *Nanoscale* **2011**, *3*, 4042.
5. Marín, M. L.; McGilvray, K. L.; Scaiano, J. C. *J. Am. Chem. Soc.* **2008**, *130*, 16572; Lanterna, A.; Pino, E.; Doménech-Carbó, A.; González-Béjar, M. *J. Pérez-Prieto Nanoscale* **2014**, *6*, 9550; Lu, X.; Rycenga, M.; Skrabalak, S. E.; Wiley, B.; Xia, Y. *Annu. Rev. Phys. Chem.* **2009**, *60*, 167.
6. Polte, J.; Ahner, T. T.; Delissen, F.; Sokolov, S.; Emmerling, F.; Thünemann, A. F. *J. Am. Chem. Soc.* **2010**, *132*, 1296.
7. Brust, M.; Fink, J.; Bethell, D. J.; Schiffrin, D.; Kielyb, C. *J. Chem. Soc., Chem. Commun.* **1995**, 1655.
8. Brust, M.; Walker, M.; Bethell, D.; Schiffrin, D. J.; Whyman, R. *J. Chem. Soc., Chem Commun.* **1994**, 801.
9. Goulet, P. J. G.; Lennox, R. B. *J. Am. Chem. Soc.* **2010**, *132*, 9582; Yu, C.; Zhu, L.; Zhang, R.; Wang, X.; Guo, C.; Sun, P.; Xue, G. *J. Phys. Chem. C* **2014**, *118*, 10434; Briñas, R. P.; Hu, M.; Qian, L.; Lymar, E. S.; Hainfeld, J. F. *J. Am. Chem. Soc.* **2008**, *130*, 975; Nakamoto, M.; Yamamoto, M.; Fukusumi, M. *Chem. Commun.* **2002**, 1622; Negishi, Y.; Nobusada, K.; Tsukuda, T. *J. Am. Chem. Soc.* **2005**, *127*, 5261; Cha, S.-H.; Kim, K.-H.; Kim, J.-U.; Lee, W.-K.; Lee, J.-C. *J. Phys. Chem. C* **2008**, *112*, 13862; Li, Y.; Zaluzhna, O.; Tong, Y. J. *Chem. Commun.* **2011**, 6033; Li, Y.; Zaluzhna, O.; Xu, B.; Gao, Y.; Modest, J. M.; Tong, Y. J. *J. Am. Chem. Soc.* **2011**, *133*, 2092; Schaaff, T. G.; Knight, G.; Shafigullin, M. N.; Borkman, R. F.; Whetten, R. L. *J. Phys. Chem. B* **1998**, *102*, 10643; Susha, A. S.; Ringler, M.; Ohlinger, A.; Paderi, M.; LiPira, N.; Carotenuto, G.; Rogach, A. L.; Feldmann, J. *Chem. Mat.* **2008**, *20*, 6169; Barngrover, B. M.; Aikens, C. M. *J. Phys. Chem. Lett.* **2011**, *2*, 990.
10. Woolridge, K.; Goncalves, L. C.; Bouzan, S.; Chen, G. *Tetrahedron Lett.* **2014**, *55*, 6362.
11. Nielsen, M. B.; Petersen, J. C.; Thorup, N.; Jessing, M.; Andersson, A. S.; Jepsen, A. S.; Gisselbrecht, J.-P.; Boudon, C. *J. Mater. Chem.* **2005**, *15*, 2599.
12. Guerro, M.; Di Piazza, E.; Jiang, X.; Roisnel, T.; Lorcy, D. *J. Organomet. Chem.* **2008**, *693*, 2345; Åxman Petersen, M.; Zhu, L.; Jensen, S. H.; Andersson, a. S.; Kadziola, a.; Kilså, K.; Brøndsted Nielsen, M. *Adv. Funct. Mater.* **2007**, *17*, 797.
13. Inagi, S.; Naka, K.; Chujo, Y. *J. Mater. Chem.* **2007**, *17*, 4122; Canevet, D.; Sallé, M.; Zhang, G.; Zhang, D.; Zhu, D. *Chem. Commun.* **2009**, 2245.
14. Andreu, R.; Cerdán, M. A.; Garín, J.; Orduna, J. *Arkivoc* **2004**, *4*, 32.
15. Au, L.; Lu, X.; Xia, Y. *Adv. Mat.* **2008**, *20*, 2517.
16. Ruff, F.; Csizmadia, I. G. *Studies in organic chemistry*, **1994**.
17. Goulet, P. J. G.; Leonardi, A.; Lennox, R. B. *J. Phys. Chem. C* **2012**, *116*, 14096; Gammons, C. H.; Yu, Y.; Williams-Jones, A. E. *Geochim. Cosmochim. Acta* **1997**, *61*, 1971.
18. Kumar, S.; Gandhi, K. S. *Ind. Eng. Chem. Res.* **2007**, *46*, 3128.
19. Jose, D.; Matthiesen, J. E.; Parsons, C.; Sorensen, C. M.; Klabunde, K. J. *J. Phys. Chem. Lett.* **2012**, *3*, 885.
20. Anema, J. R.; Li, J.-F.; Yang, Z.-L.; Ren, B.; Tian, Z.-Q. *Ann. Rev. Anal. Chem.* **2011**, *4*, 129.
21. Fracaroli, A. M.; Granados, A. M.; de Rossi, R. H. *J. Org. Chem.* **2009**, *74*, 2114.
22. Constantino, M. G.; Lacerda, V., Jr; da Silva, G. V.; Tasic, L.; Rittner, R. *J. Mol. Struct.* **2001**, *597*, 129.